Pulsating combustion of ethylene in micro-channels with controlled temperature gradient

Annalisa Di Stazio, Christian Chauveau, Guillaume Dayma, Philippe Dagaut

Pulsating combustion of ethylene in micro-channels with controlled temperature gradient

Annalisa Di Stazio[a], Christian Chauveau[a], Guillaume Dayma[a,b] and Philippe Dagaut[a]

[a]*CNRS – INSIS, 1C avenue de la Recherche Scientifique, 45071 Orléans cedex 2, France*

[b]*Université d'Orléans, Collegium Sciences et Techniques, 1 rue de Chartres, 45067 Orléans cedex 2, France*

ABSTRACT

Nowadays with the demand for high-efficiency systems, there is a growing development and application of micro electromechanical systems (MEMS devices) which may generate more energy than the modern batteries. In this context, a new experimental device has been developed. It consists of a micro tubular reactor with a controlled external temperature profile. The high gas temperature allows the auto-ignition of the mixture and the flame stabilization in reactors with inner diameter smaller than the ordinary quenching diameter. The temperature profile along the tube is measured continuously using an infrared camera while an EMCCD camera is used to collect the CH* emission from the flame. The present experimental study on C_2H_4/air mixtures reacting in narrow channels has been undertaken to provide detailed information on flame combustion at micro-scale. Three kinds of flame behaviors were observed: (i) bright and stable flames under high flow velocity, (ii) flames with repetitive extinction and ignition (FREI) in the middle flow rates range, and (iii) weak flames at low flow rates. The presence of oscillating

transitional regimes was also investigated and a detailed analysis of the unstable regimes (determination of frequencies and characteristic times) was carried out. The effect of the inlet velocity, the equivalence ratio, and the tube inner diameter were also investigated. Numerical simulations were also conducted to study the ignition characteristics of unstable flames.

1. INTRODUCTION

Micro combustion is now a very topical issue, and despite the considerable progress made in the last decade (Ju and Maruta, 2011, Kaisare and Vlachos, 2012), many aspects are still unknown. Currently, different fuels have been tested experimentally to study their ignition characteristics in micro-channels (Kamada et al., 2014, Nakamura et al., 2014, Hori et al., 2013). However, there is still a lack of clearly defined information about the dynamics of stable and unstable flames at micro-scale. As illustrated in our previous paper (Di Stazio et al., 2016), our experimental device allows to characterize the frequencies of unstable flames under various experimental conditions while ensuring a uniform temperature distribution. Moreover, the presence of oscillating flames, already observed experimentally (Di Stazio et al., 2016, Tsuboi et al., 2007) and numerically (Minaev et al., 2007, Jackson et al., 2007, Norton and Vlachos, 2003, Miroshnichenko et al., 2015), has been confirmed under specific conditions in the transitions between the different flame regimes, but the knowledge on these instabilities is still very limited.

Ethylene is one of the main intermediates in the combustion of real fuels, and thus plays a critical role in governing the kinetics and the heat release. As such, understanding its combustion behavior under micro combustion regime is crucial for the development of this combustion mode. Kikui et al. (2016) studied ethylene combustion in the weak flame regime and showed with the

help of numerical simulations that it is oxidized into formyl radicals either directly or through the formation of formaldehyde CH_2O. Furthermore, the large production of CH* radicals during ethylene combustion makes this fuel suitable for the experimental device used here.

The purpose of this work is to investigate the combustion characteristics of this key intermediate under different flame regimes (stable flames, FREI, and weak flames) as a function of the equivalence ratio. For unstable flames, the flame dynamic was characterized by a high-speed camera. This equipment allowed visualizing for the first time the spatial progression of unstable flames at high frequency. Also, the oscillating behaviors and the flame obtained under very lean conditions are discussed.

2. EXPERIMENTAL SET-UP

A schematic of the experimental setup is shown in Fig. 1 (left). C_2H_4/air mixtures were supplied in a quartz tube with an inner diameter of 1 mm at atmospheric pressure. A smaller diameter than for methane was here necessary since ethylene has a smaller quenching diameter (Gutkowski, 2006). The channel was heated externally by three H_2/O_2 flames (Spirig blowtorches) to ensure a stationary temperature profile from ambient temperature (ca. 293 K) to about 1600 K (Fig. 1, right). The temperature along the outer side of the channel was continuously measured by a FLIR A655sc thermal camera. An emissivity correction was carried out, since the emissivity of the fused silica depends on the wavelength and the temperature (Sova et al., 1998). A Princeton Instrument spectroscopy EMCCD camera, equipped with an optical band-pass filter (20BPF10-430), was used to collect the CH* chemiluminescence indicating the flame position. The acquisition frequency was set at 4260 Hz and pixel binning was performed. The signal was

amplified (high EM gain) and the spatial resolution was 62 pixels/mm. In order to track the unstable flame propagation, a high-speed camera Phantom V1611, equipped with a teleconverter Teleplus MC7, was employed. A sample rate of 12000 fps and an exposure time of 82 µs were adopted to simultaneously optimize picture brightness and temporal resolution.

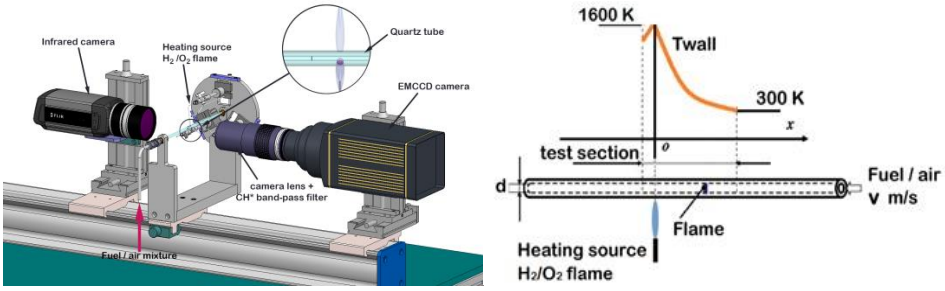

Figure 1. Left: Schematic of the experimental device; Right: Temperature profile along the channel.

3. RESULTS

- 3.1 Description of the phenomena

As previously observed (Di Stazio et al., 2016, Maruta et al., 2005) for methane/air mixtures, three flame regimes exist depending on the inlet velocity: stable flames at high speed (> 0.7 m s^{-1}), FREI (Flames with Repetitive Extinction and Ignition) for lower speeds, and weak flames at very low speed (< 0.2 m s^{-1}). In some conditions, oscillatory flames were observed between the different regimes: oscillating FREI in the transition between stable flames and FREI, and oscillating weak flames in the transition between FREI and weak flames. Results obtained over an extended range of equivalence ratios (from 0.3 to 1.5) are discussed below. Peculiar flame behaviors were observed under very lean conditions ($\varphi = 0.3$).

Figure 2 shows the variation of these different regimes when varying the equivalence ratio. As observed previously for methane/air mixtures (Di Stazio et al., 2016), the stabilization temperature of the stable flames decreases with the inlet velocity. Norton and Vlachos (2003) explained that when the inlet velocity is increased it requires a longer distance to preheat the fresh gases: the flame is therefore stabilized further downstream. The wall temperature at the flame location is thus higher and the heat losses are lower, resulting in higher reaction rates and higher flame temperatures. In the FREI regime, ignition occurs at high temperature (> 1100 K), and then the flame propagates upstream until extinction. Weak flames were observed at equivalence ratios of 1.0 and 1.5 and oscillating weak flames were observed at $\varphi = 0.9$ and 1.0. At $\varphi = 0.4$, an oscillating FREI was detected between the stable flames and the FREI regime. These oscillating regimes will be described in detail.

By comparing the results obtained for different equivalence ratios, one can notice that the minimum stabilization temperatures are obtained between $\varphi = 1.1$ and 1.3. These equivalence ratios correspond to the maximum laminar flame speed for ethylene/air mixtures.

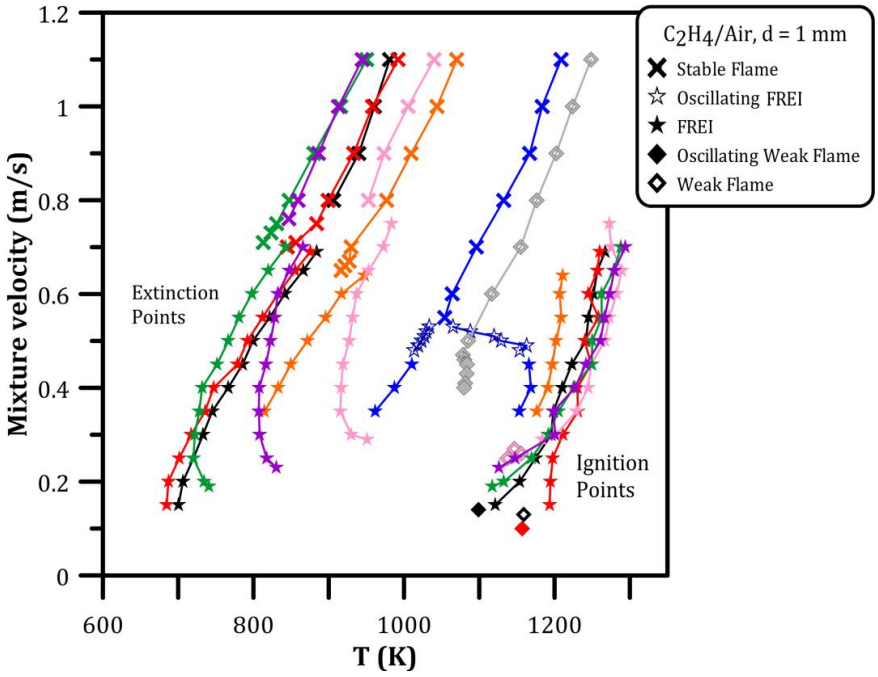

Figure 2. Flame position as a function of average inlet velocity and wall temperature as a function of the equivalence ratio: 0.3 (grey), 0.4 (blue), 0.7 (orange), 0.9 (red), 1 (black), 1.1 (green), 1.3 (purple), 1.5 (pink). (This figure is in color only in the electronic version.)

Regarding FREI, the experiments performed with the high-speed camera allowed tracking the flame inside the channel at high frequency. Figure 3 depicts the three main phases of the flame progression: ignition, propagation and time before extinction. The images obtained (top) are compared to the CH*signals recorded with the EMCCD camera (bottom). The flame ignition (a) is characterized by a low luminosity. When it propagates (b), the brightness and the thickness of the flame increase as illustrated by the CH* profile: 1.4 ms after the detected ignition, the signal is 3 mm thick. Before extinction (c), the flame gets thinner with a concave shape and the CH* profile becomes sharper with a higher intensity. The thickening of the flame front during the propagation phase cannot be attributed to an accumulative phenomenon. Experiments were also

carried out at 20000 fps and very similar flame thicknesses were observed. Images at 12000 fps were chosen in order to get higher luminosity. As compared to stable flames, one of the interests of this FREI region is that the ignition phenomenon can be observed. As can be seen from Fig. 2, fuel-lean mixtures ignite at significantly lower temperatures than stoichiometric or fuel-rich mixtures: for instance, at v = 0.4 m s^{-1}, the mixture at φ = 0.4 ignites at T = 1168K whereas the stoichiometric mixture ignites at T = 1210K.

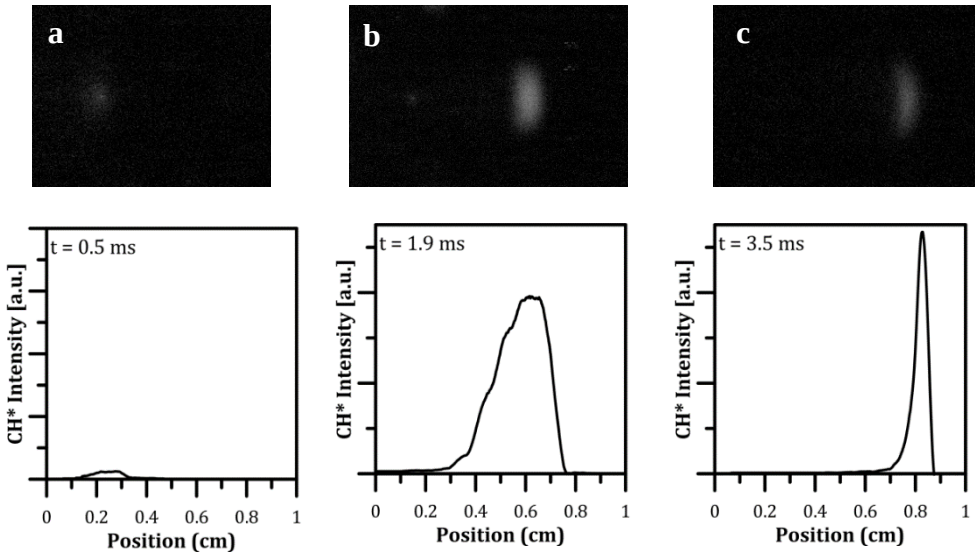

Figure 3. Flame images and corresponding CH* signals at v = 0.6 m s^{-1} and φ = 1: a) ignition, b) propagation, c) time before extinction.

The flames observed under very lean conditions (φ = 0.3) and high inlet velocity have a very low brightness, which is commonly associated with weak flames. These weak flames stabilize in the high temperature region of the temperature gradient. Decreasing the inlet velocity down to v = 0.45 m s^{-1} results in a flame stabilization at lower and lower temperatures. Then for inlet velocities below 0.45 m s^{-1}, oscillating weak flames were observed (Fig. 2). Figure 4 (left) shows

the frequency of these oscillating flames obtained through a Fourier Transform analysis of the spectral cross-section of the CH* signal. The results show that the frequency is very high but slightly decreases with the inlet velocity. The time evolution of the spatially integrated CH* signal is displayed in Fig. 4 (right). One can notice that the luminous intensity varies randomly, while for the oscillating flames observed between the stable flame and FREI regimes, the luminosity fluctuates regularly as will be detailed in Figure 5. The spatial displacement of these oscillating weak flames is of about 0.5 mm, which corresponds to a wall temperature difference of 40 K. Oscillating weak flames were also observed at equivalence ratios of 0.9 and 1.0, in the region between the FREI and the weak flame regimes.

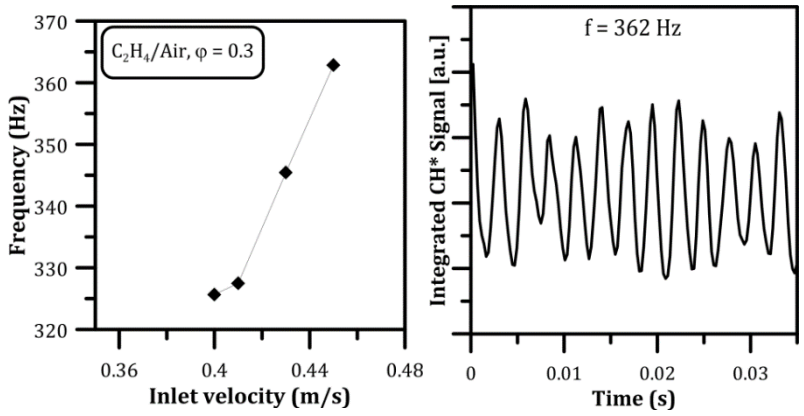

Figure 4. Left: Oscillating weak flame frequencies at φ = 0.3; Right: Temporal evolution of the integrated CH* signal at φ = 0.3 and v = 0.45 m s^{-1}.

These unstable flames are similar to FREI. Indeed, the heat released by the reaction decreases with the inlet velocity, leading to a near blow-off condition (Norton and Vlachos, 2003). The flame does not have enough energy to propagate, and stays “trapped” in the high temperature zone. During the pulsations, the radical concentration fluctuates, whereas the radical pool is

totally depleted before the re-ignition for a typical FREI, as explained by Miroshnichenko et al. (2015).

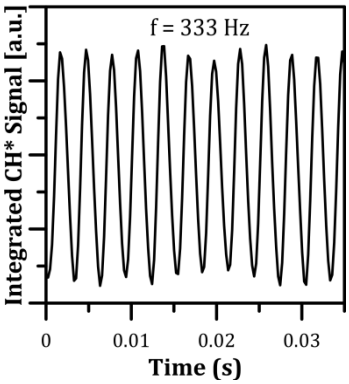

Figure 5. Oscillating flames observed at v = 0.5 m s^{-1} and φ = 0.4.

At an equivalence ratio of 0.4, oscillating flames were observed in the transition region between stable flames and FREI (Fig. 5), for average inlet velocities between v = 0.53 and v = 0.48 m s^{-1}. These oscillating phenomena start like typical FREI, but when the flames reach the temperature at which they are expected to extinguish, extinction does not occur (i.e. the CH*signal does not go to zero) and flames oscillate at high frequency. The oscillation amplitude increases when decreasing the inlet velocity until getting a typical FREI at v = 0.47 m s^{-1}. The mathematical model proposed by Jackson et al. (2007) was able to predict these instabilities that are due to the dynamic of heat losses through the tube wall.

- 3.2 Frequencies

Figure 6 shows the evolution of the frequencies obtained at different equivalence ratios. Except for oscillating phenomena, frequencies increase with the average inlet velocity. The lowest frequencies were recorded at φ = 0.9 and 1.3 at low inlet velocity (v = 0.15 m s^{-1}) while the

highest frequencies were measured at φ = 0.4. The oscillating frequencies increase as the equivalence ratio varies towards fuel-rich or fuel-lean conditions. The frequency peaks for the oscillating flames. The results were compared to those obtained for a stoichiometric methane/air mixture, with a 1 mm inner diameter tube. In this case, we observed high frequency oscillating flames in the transition between stable flames and FREI, and for a given equivalence ratio, methane/air FREI have higher frequencies.

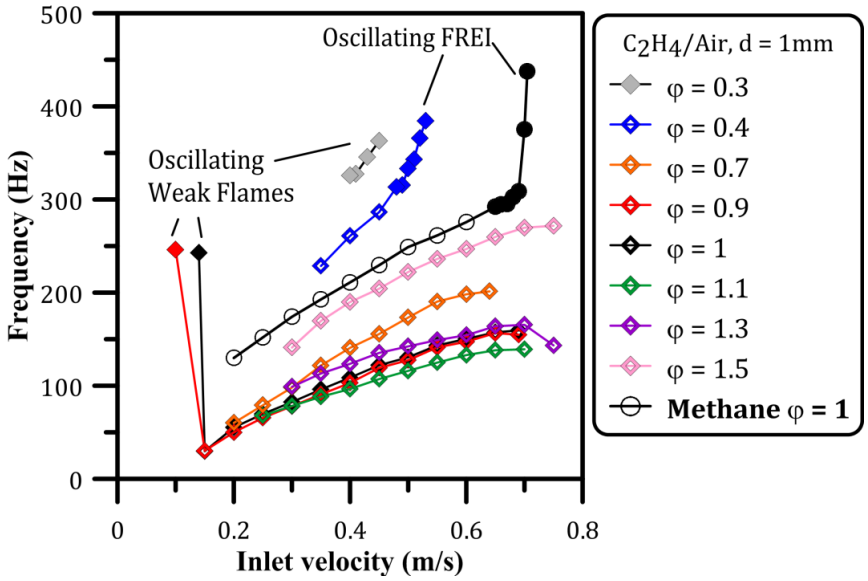

Figure 6. Flame frequencies obtained varying the average inlet velocity at different equivalence ratios. (This figure is in color only in the electronic version.)

In the case of typical FREI, the frequencies actually result in the combination of the time necessary for the flame to propagate and extinguish (time between ignition and extinction, τ_{IE}), and the time for a layer of fresh gases to reach the point where the temperature is high enough for auto-ignition (time between extinction and ignition, τ_{EI}). These two characteristic times were isolated from our experimental results and are plotted in Figure 7 as a function of the average

inlet velocity for ethylene/air mixture at φ = 1.1. From this figure, it can be seen that τ_{EI} obviously decreases when the inlet velocity increases while τ_{IE} remains approximately constant regardless of the inlet velocity, indicating that the frequency of the phenomenon is mainly driven by the advection time of fresh gases.

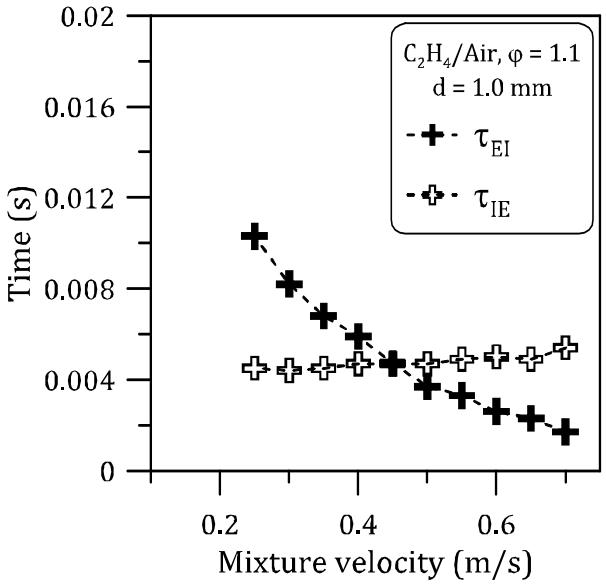

Figure 7. Evolution of the time between ignition and extinction (τ_{IE}) and the time between extinction and ignition (τ_{EI}) as a function of the average inlet velocity for ethylene/air mixture at φ = 1.1.

- 3.3 Effect of the inner diameter

The effect of the inner diameter was also investigated replacing the quartz tube of 1 mm id by a quartz tube of 0.7 mm id (the outer diameter being kept constant at 6 mm). The comparison was performed for a stoichiometric C_2H_4/air mixture and is plotted in Figure 8. As can be seen from

this figure, when the inner tube diameter decreases the FREI regime is extended towards higher average inlet velocities and ignition and extinction occur at higher temperatures. This can be directly related to the increase of the surface/volume ratio when the inner diameter is decreased: at 950 K, for instance, the heat produced in the volume of the flame in a tube of 1 mm id is greater to the heat lost to the wall through the surface of the flame, hence the flame stabilizes while, for a 0.7 mm id, heat losses decrease as r^2 whereas the heat production decreases as r^3, hence the flame extinguishes.

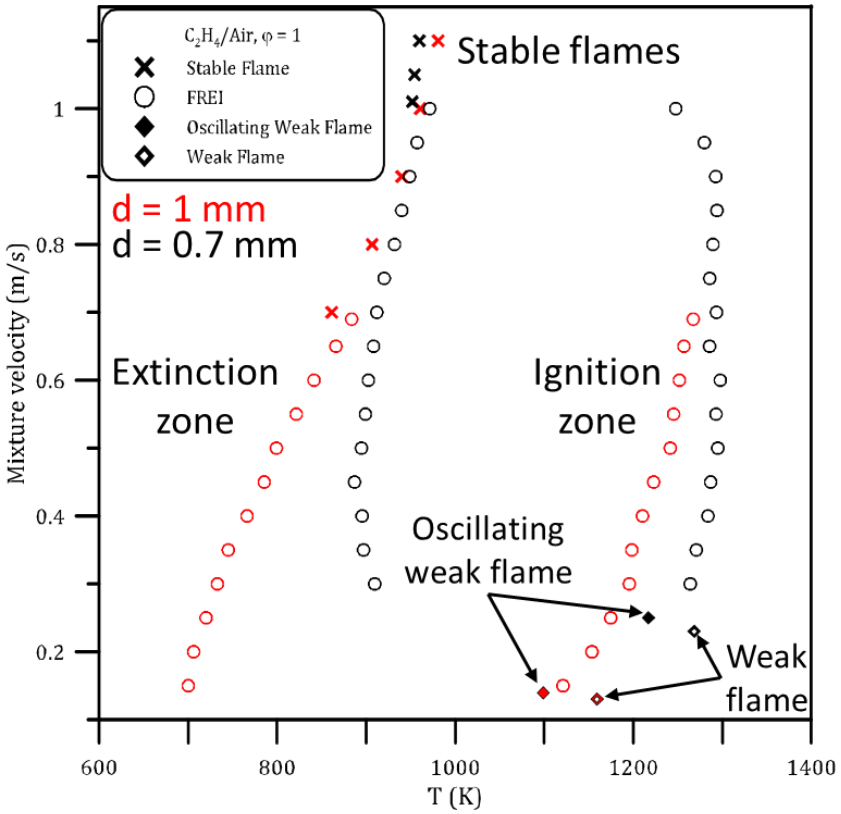

Figure 8. Effect of the inner diameter for a stoichiometric C_2H_4/air mixture. Red symbols are for 1 mm id and black symbols for 0.7 mm id. (This figure is in color only in the electronic version.)

4. MODELING

This part presents a preliminary attempt to numerically investigate the ignition phase of the conventional FREI. A 2D model was developed and tested with three detailed chemical kinetic mechanisms: GRI-Mech 3.0 (Gregory et al.), Konnov 0.5 (Konnov, 2000), and a very recent mechanism develop to predict the oxidation of C_2H_2 and C_2H_4 at high pressure (Gimenez-Lopez et al., 2016). The computations were then compared to the experimental ignition temperatures. In this 2D model, the coupled gas-phase hydrodynamics and chemical kinetics in a channel was simulated. Boundary layer approximations for compressible flow were used since there is a dominant direction along the channel and since the diffusion flux dominates the convective flux in the radial flow direction. The parabolic nature of the boundary layer equations allowed employing an explicit method of lines for the integration. An extended Von Misses transformation for which a stream function replaced the radial coordinate was also implemented. The computations were performed over 2D-axisymmetric solution domain for a cylindrical channel flows field. The solver discretized the system of equations for momentum, energy and species using finite difference approximation over uniform grid which is clustered at the outer boundary. The flow rate, temperature and species fractions at the channel inlet and the experimental wall temperature profile were given as the boundary conditions. Mixture-averaged transport properties were considered.

The numerical ignition location was defined as the spatial location for which the CH* mole fraction is maximum on the reactor centerline, in line with the definition used in the experiments. To this end, the same submechanism for CH* was added to the mechanisms when necessary.

This submechanism was taken from Konnov 0.5. CH* and CH share the same thermodynamic and transport properties. Several axial grids were tested from 5 µm to 100 µm, and an axial mesh size of 30 µm was found to be a good compromise. As well, above 6 radial meshes, the radial grid was not found to have any impact on the results. The comparison between experimental and calculated ignition temperatures was performed for a 1 mm id tube and a stoichiometric ethylene/air mixture, and is presented in Figure 9. From this figure, it can be seen that both GRI-Mech 3.0 and Gimenez-Lopez (2016) mechanisms are well able to reproduce the experimental data within the experimental uncertainty (+/- 30 K) due to the detection threshold of the EMCCD camera whereas Konnov 0.5 well captured the trend but predict an ignition temperature at much higher temperature. This discrepancy could be explained by the particular attention that was paid to the low-temperature chemistry of C_2H_5 and C_2H_3 in Gimenez-Lopez (2016) mechanism.

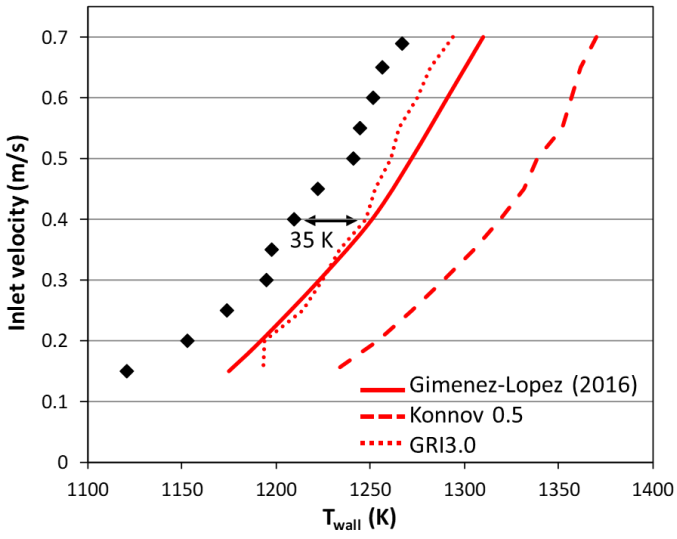

Figure 9. Comparison of the experimental (symbols) and calculated (lines) ignition temperatures for different average inlet velocities for a stoichiometric C_2H_4/air mixture in a 1 mm id tube.

5. CONCLUSIONS

Our experimental set-up confirms its interest in the study of small-scale combustion. Experiments were performed with ethylene/air mixtures in a 1 mm inner diameter tube over a wide range of equivalence ratios. Under very lean condition the combustion dynamics changed: at an equivalence ratio of 0.3, only weak flame and oscillating weak flame were observed. Furthermore, oscillating flames were observed at equivalence ratio of 0.4 between the stable flames and the FREI region. For mixtures with equivalence ratio between 1.1 and 1.3, the flames stabilize at lower wall temperatures. Furthermore, it was possible to carry out a frequency analysis, demonstrating that the highest frequencies are recorded for oscillating flames. The effect of the diameter was also investigated and showed the predominant influence of the surface/volume ratio. A modeling attempt of the ignition temperature at different average inlet velocities is also presented demonstrating the influence of the kinetics regarding this phenomenon. This experimental set-up has shown an interesting potential in the investigation of auto-ignition.

6. ACKNOWLEDGMENTS

The research leading to these results has received fundings from the European Research Council under the European Community's Seventh Framework Programme (FP7/2007–2013)/ERC grant agreement No.291049 – 2G-Csafe and from the Agence Nationale de la Recherche (ANR-12-VPTT-0008).

7. REFERENCES

DI STAZIO, A., CHAUVEAU, C., DAYMA, G. & DAGAUT, P. 2016. Combustion in micro-channels with a controlled temperature gradient. *Experimental Thermal and Fluid Science,* 73**,** 79-86.

GIMENEZ-LOPEZ, J., RASMUSSEN, C. T., HASHEMI, H., ALZUETA, M. U., GAO, Y., MARSHALL, P., GOLDSMITH, C. F. & GLARBORG, P. 2016. Experimental and Kinetic Modeling Study of C2H2 Oxidation at High Pressure. *International Journal of Chemical Kinetics,* 48**,** 724-738.

GREGORY, P., SMITH, D. M. G., FRENKLACH, M., MORIARTY, N. W., EITENEER, B. & GOLDENBERG, M. GRI 3.0. *http://www.me.berkeley.edu/gri_mech/*.

GUTKOWSKI, A. 2006. Laminar burning velocity under quenching conditions for propane-air and ethylene-air flames. *Archivum Combustionis,* Vol. 26 nr 3-4**,** 163-173.

HORI, M., NAKAMURA, H., TEZUKA, T., HASEGAWA, S. & MARUTA, K. 2013. Characteristics of n-heptane and toluene weak flames in a micro flow reactor with a controlled temperature profile. *Proceedings of the Combustion Institute,* 34**,** 3419-3426.

JACKSON, T. L., BUCKMASTER, J., LU, Z., KYRITSIS, D. C. & MASSA, L. 2007. Flames in narrow circular tubes. *Proceedings of the Combustion Institute,* 31**,** 955-962.

JU, Y. & MARUTA, K. 2011. Microscale combustion: Technology development and fundamental research. *Progress in Energy and Combustion Science,* 37**,** 669-715.

KAISARE, N. S. & VLACHOS, D. G. 2012. A review on microcombustion: Fundamentals, devices and applications. *Progress in Energy and Combustion Science,* 38**,** 321-359.

KAMADA, T., NAKAMURA, H., TEZUKA, T., HASEGAWA, S. & MARUTA, K. 2014. Study on combustion and ignition characteristics of natural gas components in a micro flow reactor with a controlled temperature profile. *Combustion and Flame,* 161**,** 37-48.

KIKUI, S., NAKAMURA, H., TEZUKA, T., HASEGAWA, S. & MARUTA, K. 2016. Study on combustion and ignition characteristics of ethylene, propylene, 1-butene and 1-pentene in a micro flow reactor with a controlled temperature profile. *Combustion and Flame,* 163**,** 209-219.

KONNOV, A. A. 2000. Detailed reaction mechanism for small hydrocarbons combustion.

MARUTA, K., KATAOKA, T., KIM, N. I., MINAEV, S. & FURSENKO, R. 2005. Characteristics of combustion in a narrow channel with a temperature gradient. *Proceedings of the Combustion Institute,* 30**,** 2429-2436.

MINAEV, S., MARUTA, K. & FURSENKO, R. 2007. Nonlinear dynamics of flame in a narrow channel with a temperature gradient. *Combustion Theory and Modelling,* 11**,** 187-203.

MIROSHNICHENKO, T., GUBERNOV, V., MINAEV, S. & MARUTA, K. Diffusive-Thermal Instabilities of High Lewis Number Flames in Micro Flow Reactor. *In:* MI, R., ed. 25th International Colloquium on the Dynamics of Explosions and Reactive Systems, 2015 Leeds (UK). 1-6.

NAKAMURA, H., TANIMOTO, R., TEZUKA, T., HASEGAWA, S. & MARUTA, K. 2014. Soot formation characteristics and PAH formation process in a micro flow reactor with a controlled temperature profile. *Combustion and Flame,* 161**,** 582-591.

NORTON, D. G. & VLACHOS, D. G. 2003. Combustion characteristics and flame stability at the microscale: a CFD study of premixed methane/air mixtures. *Chemical Engineering Science,* 58**,** 4871-4882.

SOVA, R. M., LINEVSKY, M. J., THOMAS, M. E., MARK, F. F. & THOMAS, M. E. 1998. High-temperature infrared properties of sapphire, AlON, fused silica, yttria, and spinel. *Infrared physics & technology,* 39**,** 251-261.

TSUBOI, Y., YOKOMORI, T. & MARUTA, K. Study on Ignition and Weak Flame in Heated Meso-Scale Channel. ASME 2007 International Mechanical Engineering Congress and Exposition, November 11–15, 2007 2007 Seattle, Washington, USA. Volume 6: Energy Systems: Analysis, Thermodynamics and Sustainability, 155-158.